Nonlinear hydrodynamic instability of expanding flames: Intrinsic dynamics

Guy Joulin
Laboratoire d'Energétique et Détonique, Ecole Nationale Supérieure de Mécanique et d'Aérotechnique, Site de Futuroscope, Boite Postale 109, 86960 Futuroscope Cedex, Poitiers, France
(Received 27 January 1994)

In the framework of the weak-thermal-expansion approximation, a potential flow model is employed as an analytical tool to study the dynamics of wrinkled, nearly spherical, expanding premixed flames. An explicitly time-dependent generalization of the nonlinear Michelson-Sivashinsky (MS) equation is found to control the evolution of the flame wrinkles. The new equation qualitatively accounts for the hydrodynamic instability, the stabilizing curvature effects, and the stretch of disturbances induced by flame expansion. Via a linearization and a decomposition of the flame distortion in angular normal modes, it is first shown, in agreement with classical analyses, that the above mechanisms compete at first to make the small disturbances of fixed angular shapes fade out in relative amplitude, and subsequently result in an algebraic growth. Following that, the linear response to small forcings of fixed spatial wave numbers is investigated and exponential growths are obtained. By using a separation of variables, then the pole-decomposition method, the flame evolution is converted into an N-body dynamical system for the complex spatial singularities of the front shape; an infinite number of initial condition dependent, exact solutions to the generalized MS equation are then exhibited. Each of them represents superpositions of locally orthogonal patterns of finite amplitudes which are shown to ultimately evolve into slowly varying ridges positioned at fixed angular locations. The corresponding flame speed histories are determined. Examples of nonlinear wrinkle dynamics are studied, including petal-like patterns that are nearly self-similar asymptotically in time, but in no instance could one observe a spontaneous tendency to repeated cell splitting. Open mathematical and physical problems are also evoked.

PACS number(s): 47.20.Ma, 82.40.Py, 47.54.+r

I. INTRODUCTION

As review articles [1–3] or textbooks [4,5] remind us, most of the known instabilities of premixed flames were first identified in the context of a weakly perturbed *planar* front. Among these, one may single out the hydrodynamic instability discovered by Landau [6] and Darrieus [7] because it is almost always potentially important when fast enough flames and long wavelengths are concerned. In the geometrical framework of a nearly planar flame, Sivashinsky [8] was even able to get a good insight into the dynamics of wrinkles of finite amplitude, when wrinkling is solely due to the Landau-Darrieus instability; his analysis (see also Ref. [9]) led to the so-called Michelson-Sivashinsky (MS) equation which, in its one dimensional standard form, reads as

$$\phi_\tau+\tfrac{1}{2}\phi_X{}^2=\mu\phi_{XX}+I(\phi,X)\ ,\qquad I(\phi,X)\equiv\frac{1}{\pi}\fint_{-\infty}^{\infty}\frac{\phi_X(\tau,Z)}{X-Z}dZ \tag{1.1}$$

(τ, X, and ϕ, respectively, represent reduced time, transverse coordinate, and flame shape; $\mu>0$ is a constant coefficient; and the subscripts denote partial derivatives). A formally identical equation previously cropped up in plasma physics [10] and the overall properties of its solution were first investigated numerically in that context [11]. Upon numerical integration with periodic boundary conditions [12], (1.1) often ultimately leads to a steady flame shape with the maximum available wavelength, even when the wavelength markedly exceeds that of the most amplified small disturbance of a plane flame. This somewhat paradoxical result can be explained by a mechanism first proposed by Zel'dovich *et al* [13], and soon extended to other curved interfaces [14,15]. The local disturbances of a steady curved flame are indeed shifted by the geometry-induced, or real, nonhomogeneous advection along the front, while their wavelengths (hence their growth rates) are modified by local tangential stretch. As a result, steady curved flames in a tube or the large-scale steady solutions relative to the MS equation may be linearly stable though they are locally nearly planar. The above theory and its numerical confirmation [16] devoted to the MS equation show that the model of a planar flame, though sufficient in enabling us to understand the local instability mechanisms, is too restrictive to capture the wrinkle fate; in the limit of long times the local flame dynamics is affected, if not driven, by the *large-scale front geometry*. Thus, a strong motivation existed for studying in detail generalizations of the MS equation pertaining to other large-scale geometries.

As for nearly *parabolic*, perturbed flame shapes, a step in this direction has been made [17]. In the linear domain, quantitative agreement with the numerical results of Denet [16] has been obtained; furthermore, nonlinear analogs of the WKB results of Zel'dovich *et al.* [13] have been displayed analytically, after study of a generalized version of the MS equation which formally differed from (1.1) by the inclusion of a convectivelike term $SX\phi_X$, with $S>0$, on the left hand side. The latter

did reinforce the conclusion that the overall geometry is a very important ingredient of flame dynamics; if strong enough, the wavelength stretch may lead to metastability phenomena, the consequences of which show up as secondary randomlike subwrinkles in numerical (hence necessarily slightly noisy) integrations of (1.1) when the integration domain is wide enough [18]. Despite the aforementioned investigations, however, one is not yet able to understand the overall dynamics of all weakly curved, evolving flames; the statement is *a fortiori* true if propagations in fluctuating media are thought of.

The present paper details with the case of nearly *spherical,* expanding flames which, at least apparently, are the most simple *evolving* structures. As is well known, this model is quite attractive because of its symmetry and because the flame surface is closed; in addition, this geometry can be obtained fairly accurately in experiments when the initial mixture is quiescent and ignition is triggered by a localized energy deposit [19,20]. This geometrical framework also seems to be a good starting point in investigating the expansion of closed flames in moderately turbulent flows, a phenomenon that one ought to understand for fundamental [19] as well as practical [21] reasons, not to mention the safety considerations.

It is not that one ignores everything about the stability of spherically, expanding flames. On the contrary, the pioneering normal-mode linear analysis of Istratov and Librovich [22] and the more accurate one recently performed by Bechtold and Matalon [23] have shown that the time-dependent stretch induced by expansion does alter the dynamics of disturbances of small amplitude. This is due to a linear increase of their wavelength with time, and any disturbance of a given angular shape first decays in amplitude (relative to the flame radius) and then ultimately grows algebraically. In addition, the aforementioned studies identified a particular angular mode, the relative amplitude of which has the shortest period of decay; presumably, it should correspond to the one that is observed at the threshold of instability. In fact, though quite accurate, the most recent analyses of this kind markedly underestimate the flame radius at the visual onset of the instability and the rank of the angular harmonics involved at this instant [20]. The effect of finite amplitudes has been invoked [5] to account for this kind of discrepancy, but no thorough investigation is yet available.

To progress in this problem, further nonlinear studies may be warranted; the present paper is an attempt in that direction. Upon use of the weak-thermal-expansion approximation [8], a time-dependent generalization of the MS equation is first derived which formally differs from (1.1) by the inclusion of a convectivelike term $X\phi_X/\tau$ on the left hand side. In the linear domain, results that are qualitatively similar to the previously referred to normal-mode analyses of expanding flames are found. The linear flame response to external disturbances of fixed spatial wavelength is then considered, and exponential growths, hence ultimately faster than the algebraic ones, are predicted.

Furthermore, the MS equation (1.1) and its two aforementioned generalizations share a useful property in the nonlinear domain, namely, by using the pole-decomposition method, an infinite number of exact, finite-amplitude solutions can be found for each of them. Presumably invented for the Korteweg–de Vries (KdV) equation [24] and later adapted to various other models [25,26], the method allowed Thual, Frisch, and Henon [27] to solve the MS equation (1.1) and to explain structures previously revealed by numerical means only; the corresponding increase in flame speed which is induced by the instability also turned out to be easily accessible [28]. Here, we employ the same approach to analyze how finite-amplitude disturbances of a steadily expanding flame spontaneously evolve. It will be shown that, despite information obtained in the present article, this seemingly simple problem still remains somewhat puzzling. It seems more and more plausible, however, that externally induced disturbances play a crucial role.

When this paper was in its final stage of preparation, this author became aware of the interesting related research undertaken by Filyand, Sivashinsky, and Frankel [47]. Specifically, the authors of [47] considered the dynamics of nearly cylindrical expanding flames by means of a model evolution equation for the flame shape, which is structurally similar to that derived in the present paper [Eq. (7.2)], and then integrated it numerically by a pseudospectral method. They found that small random initial corrugations first evolve to a few ridges which stay angularly fixed; then at a late stage (about 35 times the time singled out by an analysis à la Istratov-Librovich [22]; see Sec. VI A) the front becomes suddenly covered with small-scale cells and ultimately undergoes a progressive fractalization.

The paper is organized as follows: Sections II and III are, respectively, devoted to posing the problem and to choosing the orders of magnitude involved in the small-expansion approximation. The evolution equation is then obtained (Sec. IV) and its symmetric solution introduced (Sec. V). In Sec. VI linear analyses of stability and response are reported and discussed. The pole-decomposition method is presented (Sec. VII) and its consequences are analytically studied in different situations (Secs. VIII, IX, and X). After presenting preliminary numerical results on pole motions (Sec. XI), concluding remarks are made and some open problems are evoked (Sec. XII).

II. MODEL AND BASIC EQUATIONS

The present paper is devoted to wrinkled flames expanding from a center (Fig. 1). A key grouping in our analysis is the density contrast γ built upon the unburned gas density (ρ_u) and that of the burned medium ($\rho_b < \rho_u$): $\gamma = (\rho_u - \rho_b)/\rho_u$. We will formally consider γ as a small parameter, even though realistic values are of about 0.8 ($\rho_u = 5\rho_b$), because the small-γ limit is the only systematic procedure available to us to study the evolution of wrinkles of finite amplitudes analytically while still retaining the Landau-Darrieus instability mechanism which $\gamma > 0$ brings about. Furthermore, it gave qualitatively good results in the case of nearly planar fronts

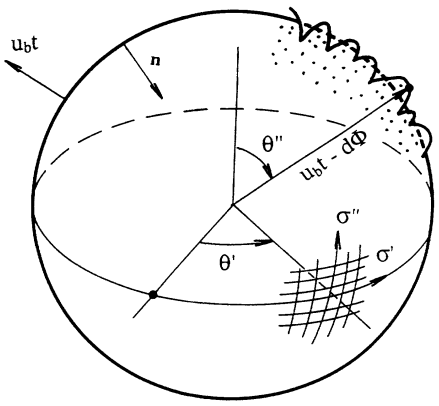

FIG. 1. Sketch of expanding flame and coordinate systems.

[8,29]. The main simplifications brought about by the assumption $\gamma \ll 1$ can be summarized as follows.

(i) The induced flow field disturbances by wrinkling are *potential* to leading order in γ on both sides of the flame front [8,9].

(ii) the Landau-Darrieus instability is weak (it disappears when $\gamma=0$) so that the stabilizing influence of nonlinearity already operates when the wrinkles have an $O(\gamma)$, hence small, amplitude compared to their wavelength [8]. A weakly nonlinear analysis is then adequate.

(iii) Once again due to the weakness of the Landau-Darrieus instability, the dependency of the local flame speed upon local front curvature [30,31] confines this instability to a range of wavelengths that are long compared to the flame thickness $d=D_{\rm th}/u_L$ based upon the thermal diffusivity $D_{\rm th}$ of the fresh mixture and the laminar burning speed u_L.

On a more practical level this means that, in the small-γ limit, one can qualitatively capture the consequences of the hydrodynamical instability by considering a weakly wrinkled flame surface separating piecewise-incompressible media in which potential flows prevail, and which propagates itself at a curvature-dependent velocity into the fresh medium. Of course, as (i)–(iii) only hold when $\gamma \ll 1$, the dynamics obtained in this manner must be specialized to the small-γ limit for sake of consistency. More specifically, we write the velocity field $\mathbf{u}$ as

$$\mathbf{u}=\text{grad}V\ , \tag{2.1}$$

where, because of piecewise incompressibility and the continuity equation, $\text{div}\mathbf{u}=0$, the velocity potential V satisfies

$$\nabla^2 V=0\ . \tag{2.2}$$

In the case of flames that expand approximately radially from about the origin ($r=0$) of the coordinates (Fig. 1), V will vanish at infinity ($r=\infty$) if, as we assume here, the fresh medium is at rest at the initial time $t=0$. Furthermore, because of the gas expansion across the flame, $V(\mathbf{r},t)$ undergoes a jump in normal gradient, whereas V itself and its tangential gradient are continuous. At a level of accuracy compatible with a leading order analysis in the small-γ limit, it is enough to assume [9]

$$[\mathbf{u}\cdot\mathbf{n}]=u_L\frac{\gamma}{1-\gamma}\ , \tag{2.3}$$

$$[\mathbf{u}\cdot\mathbf{t}]=0\ , \tag{2.4}$$

where $\mathbf{t}$ is any tangent vector to the front, $\mathbf{n}$ is the unit normal vector pointing towards the burned gases, and the notation $[f]$ means

$$f(\text{burned side})-f(\text{fresh side})\ .$$

Equations (2.3) and (2.4) correspond to the continuity and tangential momentum balances across a thin flame, respectively.

Once complemented with the requirement of boundedness of V at the origin (there is no source or sink of fluid), Eqs. (2.1)–(2.4) allow one to compute V and then $\mathbf{u}$ for any prescribed flame shape. The latter is constrained by the kinematic relationship

$$\mathbf{n}\cdot(\mathbf{u}-\mathbf{D})_{\rm fresh}=u_L[1-\mathcal{L}(1/R_1+1/R_2)]\ , \tag{2.5}$$

which involves the flame velocity $\mathbf{D}$, the local curvature $(1/R_1+1/R_2)$ of the front (taken >0 for an expanding spherical flame). The proportionality coefficient ($\mathcal{L}$) between curvature and local changes in normal burning speed $\mathbf{n}\cdot(\mathbf{u}-\mathbf{D})_{\rm fresh}$ is the so-called Markstein length [30]. It is taken positive, is essentially proportional to the actual thickness (d) of the front, and is supposedly known in advance for each mixture, from measurements [32] or analyses of the inner flame structure [31]; typically, $\mathcal{L}/d$ ranges from 4 to 8 for usual hydrocarbons burning in air [32,33].

III. ORDERS OF MAGNITUDE

We found it convenient to introduce scaled variables of order unity which will automatically specialize the resolution of (2.1)–(2.5) and the corresponding results to the limit $\gamma\to 0^+$.

A. Space scales

Studying nearly flat flames for $\gamma \ll 1$ revealed that both the marginally stable and the most rapidly growing flame shape disturbances have $O(d/\gamma)$ wavelengths [7]. We shall assume that the relevant wrinkles still have this size. As a consequence, the range of hydrodynamic disturbances due to wrinkling corresponds to a strip of $O(d/\gamma)$ width about the front; then, it is natural to introduce the new radial coordinate ξ by

$$r=u_b t+2d\xi/\gamma\ ,\quad u_b\equiv u_L/(1-\gamma)\ , \tag{3.1}$$

where the factor of 2 is used for future convenience and the first term on the right hand side of (3.1) is the radius of a flame expanding at a constant velocity.

B. Time scale

Over the range of $O(d/\gamma)$ wrinkle wavelengths, the growth rate pertaining to nearly planar fronts is

$O(\gamma^2 u_L/d)$. Accordingly, we shall employ

$$\tau = t u_L \gamma^2/4d \tag{3.2}$$

as $O(1)$ reduced time (the factor of 4 is also here for future convenience). For $\tau = O(1)$, the flame radius r is $O(d/\gamma^2)$ and hence large compared to the width of the layers corresponding to $\xi = O(1)$ and to the flame front thickness d. This justifies self-consistently why we employ results from nearly planar flames in estimating the scales involved.

C. Angles

From the $O(d/\gamma^2)$ flame radius and the $O(d/\gamma)$ wavelengths, one deduces that $O(\gamma)$ ranges of polar angles θ', θ'' are involved. To avoid the artificial singularities brought about by an arbitrary choice of coordinate orientation near the north and south poles of spherical coordinates, one is lead to focus on a patch of flame front near the equator (Fig. 1) and to introduce the scaled angles

$$(\sigma', \sigma'') = 2(\theta', \theta'' - \pi/2)/\gamma \ . \tag{3.3}$$

D. Amplitude of wrinkling

The flame front will be described by the representation

$$r = u_b t - d\Phi(\tau, \sigma', \sigma''; \gamma) \tag{3.4}$$

(i.e., $2\xi = -\gamma\Phi$) so that $\Phi > 0$ corresponds to the burnt side. As indicated in the pioneering work of Sivashinsky [8], the dominant nonlinearity is that brought about by Huygens' propagation (i.e., by the difference between $\mathbf{n}\cdot\mathbf{D}$ and $-\mathbf{r}\cdot\mathbf{D}/r$), and it manifests itself when the wrinkles have an $O(\gamma)$ amplitude to wavelength ratio. We are thus led to anticipate that

$$\Phi(\tau, \sigma', \sigma'', \gamma) = \Phi(\tau, \sigma', \sigma'') + o(1) \ , \tag{3.5}$$

where $\Phi(\tau, \sigma', \sigma'') = O(1)$ in the limit $\gamma \to 0^+$.

E. Flowfield disturbances

When curvature effects are absent ($\mathcal{L}/d = 0$), Eqs. (2.2)–(2.4) admit a spherically expanding flame of constant velocity $[r = u_L t/(1-\gamma)]$, which corresponds to a potential $\bar{V} = \text{const}$ in the burned gases and to $\bar{V} = -u_L^3 \gamma t^2/r(1-\gamma)^3$ outside. On the other hand, it is known from the original analyses of Landau [6] and Darrieus [7] that the velocity disturbances due to a wrinkle of $O(d)$ amplitude and $O(d/\gamma)$ wavelength is $O(u_L \gamma^2)$. One is thus led to write

$$V = \bar{V}(r, t) + u_L \gamma \, dw(\tau, \sigma', \sigma'', \xi) + o(\gamma d) \ , \tag{3.6}$$

where $w = O(1)$.

IV. THE EVOLUTION EQUATION

Once the scalings (3.1)–(3.5) are introduced, the evolution equation for $\Phi(\tau, \sigma', \sigma'')$ could be deduced from the result of Frankel [53], which is valid for any closed flame surface separating potential burnt-unburnt flows and any γ. For the sake of completeness, a direct derivation of the results pertaining to the small-γ case is outlined below. When Eqs. (3.1)–(3.6) are plugged into (2.1)–(2.4) and only the leading order in γ is retained, one arrives at the differential equation

$$\frac{\partial^2 w}{\partial \xi^2} + \frac{1}{\tau^2}\left[\frac{\partial^2 w}{\partial \sigma'^2} + \frac{\partial^2 w}{\partial \sigma''^2}\right] = 0 \ , \tag{4.1}$$

the solution of which has to fulfill the boundary conditions

$$|w| < \infty \ , \tag{4.2}$$

$$w = 0 \ \text{ at } \ |\xi| = \infty \tag{4.3}$$

and

$$\left[\frac{\partial w}{\partial \xi}\right]_-^+ = 0 \ , \tag{4.4}$$

$$[\mathbf{t}\cdot\nabla w]_-^+ = -\mathbf{t}\cdot\left[\frac{\partial \Phi}{\tau \partial \sigma'} \ , \frac{\partial \Phi}{\tau \partial \sigma''}\right] \ , \tag{4.5}$$

where $[f]_-^+$ denotes $f(\xi = 0^+) - f(\xi = 0^-)$. The above system is easily solved upon use of Fourier transforms with respect to σ' and σ''. It is even simpler to notice that σ'/τ and σ''/τ play the same role as transverse Cartesian coordinates $X = \sigma'/\tau$ and $Y = \sigma''/\tau$ did in the study of nearly planar wrinkled flames [7]; one can therefore immediately transpose the results of Ref. [7] to obtain the following expression for the velocity disturbance U^+ induced by flame wrinkling just ahead of the front itself:

$$U^+ = -\frac{1}{\tau} I(\Phi, \boldsymbol{\sigma}) \ , \tag{4.6}$$

where the linear operator $I(\ , \boldsymbol{\sigma})$ is defined in terms of each angular mode $e^{i\mathbf{K}\cdot\boldsymbol{\sigma}}$, $\boldsymbol{\sigma} = (\sigma', \sigma'')$ by

$$I(e^{i\mathbf{K}\cdot\boldsymbol{\sigma}} \ , \boldsymbol{\sigma}) \equiv K e^{i\mathbf{K}\cdot\boldsymbol{\sigma}} \ , \tag{4.7}$$

with $K \equiv (\mathbf{K}\cdot\mathbf{K})^{1/2}$; for functions which depend only on one space coordinate, $I(\ )$ has the explicit representation shown in (1.1). Now that U^+ is expressed in terms of Φ, one only has to combine it with the leading order of the kinematic relationship (2.5), viz.,

$$\Phi_\tau + \frac{1}{2\tau^2}|\nabla\Phi|^2 = \frac{\mu}{\tau^2}\Delta\Phi + \frac{2\mu}{\tau} - U^+ \ , \tag{4.8}$$

to obtain the sought after evolution equation for $\Phi(\tau, \boldsymbol{\sigma})$,

$$\Phi_\tau + \frac{1}{2\tau^2}|\nabla\Phi|^2 = \frac{\mu}{\tau^2}\Delta\Phi + \frac{1}{\tau} I(\Phi, \boldsymbol{\sigma}) + \frac{2\mu}{\tau} \ . \tag{4.9}$$

Here, $\mu \equiv \mathcal{L}/d$ is the Markstein number, Δ stands for $\partial^2/\partial\sigma'^2 + \partial^2/\partial\sigma''^2$, τ as a subscript is a derivative, and $\nabla = (\partial/\partial\sigma', \partial/\partial\sigma'')$. As claimed previously, the dominant nonlinearity featuring in this time-dependent MS equation has a purely eikonal origin and it comes from expanding the nearly radial unit vector $\mathbf{n}$ about $-\mathbf{r}/r$ [see (4.8)]. The following sections (V–XI) of this paper are devoted to studying (4.9).

V. THE SYMMETRIC SOLUTION

When the angular dependence of Φ is absent, one has

$$\Phi_\tau = 2\mu/\tau \ . \tag{5.1}$$

The right hand side of (5.1) gives the influence of the unperturbed front curvature upon the local flame velocity and is nothing but the small-γ residual of the effect quantified by Bechtold and Matalon [23] in the $\gamma = O(1)$ case. As we now known it [31,33], the Markstein number μ' pertaining to be burned gas flame speed is not the same [for $\gamma = O(1)$] as that (μ) based upon the fresh mixture, because of accumulation effects within the flame front itself which possesses a finite, even if small, thickness. When premixtures of air and ordinary fuels (with the exception of H_2) are used, the latter Markstein length is almost always positive, whereas the former may be negative. This numerical difference, unfortunately, disappears in the limit $\gamma \to 0$. Nevertheless, so as to increase the flexibility of the model and to account qualitatively for the aforementioned difference in Markstein lengths, we shall allow the right hand side of (5.1) and the last term in (4.9) to be written as $2\mu'/\tau$, where μ' may have any sign. This will help us formally distinguish between the influence of the mean curvature upon the flame speed and that due to wrinkling.

VI. LINEAR STABILITY ANALYSES

A. Angular normal modes

Provided that the flame shape disturbances are small enough, Eq. (4.9) can be linearized about the purely radial solution. One may then focus on a single angular mode. Specifically, one writes

$$\Phi(\sigma',\sigma'',\tau) - 2\mu' \ln\frac{\tau}{\tau_0} = \mu\Gamma(\tau)\exp(in\sigma' + im\sigma'') \ll 1 \ , \tag{6.1}$$

where the "harmonic numbers" n and m may take any real $O(1)$ value [the spherical patch corresponding to $\sigma',\sigma'' = O(1)$ is rather arbitrary in exact size], $\tau_0 > 0$ is some initial time, and the small amplitude $\Gamma(\tau)$ is given by

$$\dot{\Gamma} = \Gamma(|K|/\tau - \mu K^2/\tau^2) \ , \quad K^2 \equiv m^2 + n^2 \ . \tag{6.2}$$

One may note that $q \equiv |K|/\tau$ plays the role of an instantaneous wave number; that $q(\tau) \sim 1/\tau$, of course, is a consequence of the wavelength stretching induced by expansion. Equation (6.2) is integrated into

$$\Gamma(\tau)/\Gamma(\tau_0) = \left[\frac{\tau}{\tau_0}\right]^{|K|} \exp\left[\mu K^2\left[\frac{1}{\tau} - \frac{1}{\tau_0}\right]\right] \ , \tag{6.3}$$

where $\Gamma(\tau_0)$ is the initial amplitude. The nonexponential growth of Γ also is due to $q \sim 1/\tau$; if curvature effects were neglected ($\mu = 0$) the growth rate should indeed have the form $\dot{\Gamma}/\Gamma \sim q$, as dimensional arguments show it [6].

At this stage of our investigation, one may introduce an argument due to Istratov and Librovich [22]. In order that a disturbance may be seen as cropping "out" of an expanding spherical front, its amplitude must grow faster than the mean flame radius does. This leads to the notion of a *relative amplitude* $C(\tau) \equiv \Gamma(\tau)/\tau$, the evolution of which is given by

$$\dot{C} = C[(|K| - 1)/\tau - \mu K^2/\tau^2] \tag{6.4}$$

or, explicitly, by

$$C(\tau)/C(\tau_0) = \left[\frac{\tau}{\tau_0}\right]^{|K|-1} \exp\left[\mu K^2\left[\frac{1}{\tau} - \frac{1}{\tau_0}\right]\right] \ . \tag{6.5}$$

In a sense, the mean flame radius growth suppresses the long-wave instability corresponding to $|K| < 1$, even though $\Gamma(\tau, |K| < 1)$ grows limitlessly with time. Equation (6.5) is plotted in Fig. 2. When $|K| > 1$, $C(\tau)$ first fades out, as a result of initially strong local curvature effects ($q \sim 1/\tau$); $C(\tau)$ is then predicted to grow, as a result of a Landau-Darrieus instability which has a weaker and weaker "strength" ($q \sim 1/\tau$), but is never negligible since $q(\tau) \sim 1/\tau$ is not integrable at $\tau = \infty$. The transition $\dot{C} = 0$ occurs at a time τ_K defined by

$$\tau_K = \mu K^2/(|K| - 1) \ . \tag{6.6}$$

One first notes that $\tau_K \cong \mu|K|$ when $|K| \gg 1$. In other words, the disturbances of high enough harmonic numbers (K) start to grow (in terms of C) when τ exceeds a value which is roughly proportional to $|K|$ itself so that the corresponding spatial wave number $K/\tau_K \cong 1/\mu$ corresponds to the nontrivial marginal mode of the linearized MS equation. This is usually viewed as the root of the cell-splitting phenomenon, which is often ultimately observed experimentally when the flame radius gets large enough [20,34], because the newly growing disturbances would have a constant wavelength, whereas the flame perimeter steadily increases. We next note that $\tau_K \sim \mu$, so that the appearance of instabilities is expected to be delayed as the Markstein constant is increased. However, since different K's yield different rates of growth [$C(\tau \gg \mu|K|) \sim \tau^{|K|-1}$], the linear theory does not indicate how a phenomenon of cell splitting would manifest itself. Equation (6.6) also shows the existence of an abso-

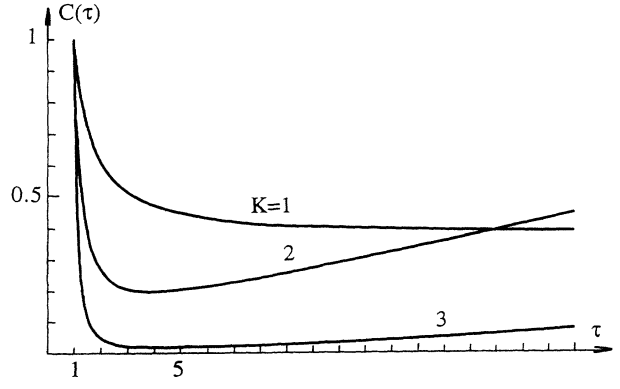

FIG. 2. Evolution of relative amplitude of disturbance $C(\tau)$ as given by the linear equation (6.5).

lute minimum $\tau_*=4\mu$ of τ_K, which is attained for $|K|=K_*\equiv 2$ (Fig. 3) and which coincides with the shortest growth time of disturbances in almost planar configurations. If present at the initial times with a nonzero amplitude, this particular mode should be the first to be observed as a growing disturbance; accordingly, $\tau=\tau_*$ should correspond to the onset of the instability, if Istratov and Librovich's criterion is correct.

One may thus say that the linearized version of (4.9) qualitatively reproduces the same results (and hence presumably has the same drawbacks) as the analyses of [22,23], due to the structure of $\dot{C}/C$ which the two latter theories share with (6.4) itself for disturbances of high enough harmonic numbers. Hopefully, the nonlinear version (4.9) will help us understand qualitatively why the aforementioned studies, though accurate in the linear domain, do not quantitatively reproduce the experimental results on the onset of instability.

B. Linear response

What was done in Sec. VI A only dealt with initial value problems for which each *angular*-mode amplitude Γ was assumed given at $\tau=\tau_0$. However, especially in the context of a theory of turbulent expanding flames, it would also be quite interesting to study the linear response of a spherical flame to an external noise, e.g., of hydrodynamical origin, which would exhibit a fixed wavelength. To this end, we now consider a *nonhomogeneous,* linearized version of (4.9), viz.,

$$F_\tau=\frac{\mu}{\tau^2}\Delta F+\frac{1}{\tau}I(F,\sigma',\sigma'')+2\mu'/\tau+u_e\exp(i\omega_e\tau+ik_e\sigma'\tau)\ . \tag{6.7}$$

The last term in the right hand side, a single-mode forcing, represents a fluctuating radial velocity component with intensity $u_e>0$, frequency ω_e, and fixed *spatial* wave number $k_e>0$. For simplicity, the "noise" is assumed to be "independent of σ," so that F may depend only on τ and σ'. Equation (6.7) is then fourier transformed $[\sigma'\Longleftrightarrow K,\ F(\tau,\sigma')-2\mu'\ln\tau\Longleftrightarrow\psi(\tau,K)]$ to yield

$$\psi_\tau=\psi\left[\frac{|K|}{\tau}-\frac{\mu K^2}{\tau^2}\right]+u_e e^{i\omega_e\tau}\delta(K-k_e\tau)\ . \tag{6.8}$$

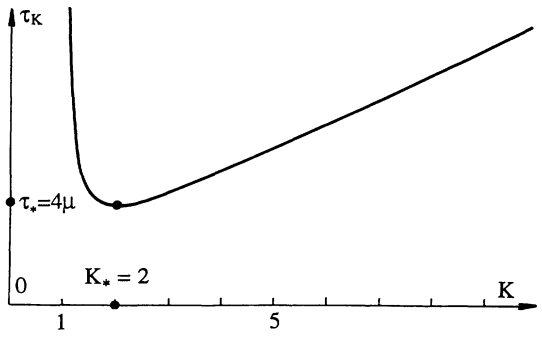

FIG. 3. The time τ_K at which the relative amplitude $C(\tau)$ of an infinitesimal normal mode reaches its minimum vs angular harmonic number K [Eq. (6.6)].

Since only the flame response is needed here, we assume that $\psi(\tau=0,K)=0$; the solution to (6.8) then has the form

$$\psi=e^{\mu K^2/\tau}\tau^{|K|}\int_{0^+}^{\tau}u_e e^{i\omega_e Z}\delta(K-k_eZ)\times e^{-\mu K^2/Z}Z^{-|K|}dZ\ , \tag{6.9}$$

or, equivalently,

$$\psi=\frac{u_e}{k_e}e^{i\omega_eK/k_e}\left[\frac{\tau k_e}{K}\right]^{|K|}e^{+\mu K^2/\tau-\mu Kk_e}\ , \tag{6.10}$$

as $\delta(Z)=\delta(-Z)$ and $\delta(aZ)=|a^{-1}|\delta(Z)$. Because $\tau>0$ and $k_e>0$, the above expression is only valid for $0^+<K<k_e\tau$; otherwise, $\psi\equiv 0$. That $\psi\equiv 0$ for $K>k_e\tau$ is a logical finding, for the above analysis of flame response is linear and the only spatial wave numbers which may then contribute to the flame shape are stretched versions of k_e. If the noise is switched on at τ_0, the results (6.10) and (6.11) only hold for $k_e\tau_0<K<k_e\tau$; otherwise, $\psi=0$. The above equation is best interpreted in terms of the Fourier transform of

$$\phi(X,\tau)\equiv F(X/\tau,\tau)-2\mu'\ln\tau\ ;$$

again, $X=\sigma\tau$ represents an arclength and k denotes the corresponding (spatial) wave number. Given the definition of a Fourier transform, $\psi(\tau,k\tau)$ represents the *spatial* Fourier transform of the *relative* disturbance amplitude $\phi(X,\tau)/\tau$. From (6.10) one deduces that

$$|\psi(\tau,k\tau)|=\frac{u_e}{k_e}e^{k_e[\kappa\ln 1/\kappa-\mu k_e\kappa(1-\kappa)]\tau}\ , \tag{6.11}$$

where $0<\kappa\equiv k/k_e<1$. Equation (6.11) is reminiscent of the results deduced from the "usual" MS equation, which would imply that the $2\pi/k_e$-periodic, externally excited disturbances of a planar flame have an amplitude $\Gamma(\tau)$ given by

$$\Gamma(\tau)\sim\mu u_e e^{k_e(1-\mu k_e)\tau}\ , \tag{6.12}$$

when $\mu k_e<1$. Comparing (6.12) and (6.11) shows that the expansion somehow "dresses" in different ways the respective contributions of curvature and of hydrodynamics to the overall rate of growth of the energy distribution. According to (6.11), for a given k_e the modes which are the fastest to grow "out" of the expanding flame as $\tau\to\infty$ correspond to $\kappa\cong\kappa_m$, where κ_m is associated with the maximum exponent in (6.11) (see Fig. 4). κ_m is given by the smaller root of the following transcendental equation:

$$1+\ln\kappa_m+\mu k_e(1-2\kappa_m)=0\ , \tag{6.13}$$

to be solved with the constraint $0<\kappa_m<1$ [if (6.13) has two roots less than unity, the larger one yields a minimum of ψ]. Once κ_m is computed, the corresponding value (k_m) of k is available, thereby giving the (k_e,k_m) curve in a parametric form, viz.,

$$\mu k_e=-(1+\ln\kappa_m)/(1-2\kappa_m)\ ,\quad \mu k_m=\kappa_m(\mu k_e)\ ,\quad 0<\kappa_m<1\ . \tag{6.14}$$

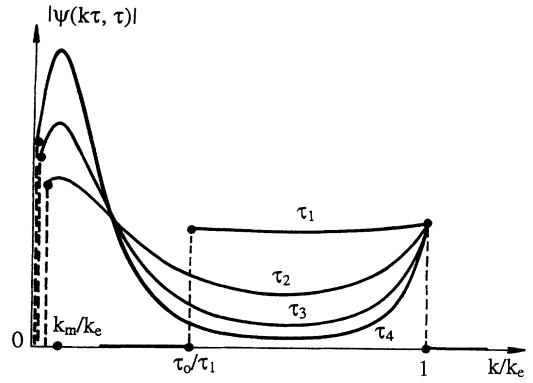

FIG. 4. Snapshots of the power density spectrum of wrinkling $|\psi(k\tau,\tau)|$ when the harmonic forcing is switched on at $\tau_0>0$, $\tau_0<\tau_1\cdots<\tau_4$.

Because $k_e>0$ and $\kappa_m<1$, Eq. (6.14) implies $k_m<k_e/e$, in any case. For $\mu k_e\gg 1$, Eq. (6.14) gives

$$\mu k_m = e^{-1}\mu k_e \exp(-\mu k_e) \ll 1 ,$$

whereas the opposite limit $\mu k_e \ll 1$ leads to $\mu k_m = e^{-1}\mu k_e \ll 1$. The curve defined by (6.14) is plotted in Fig. 5. It yields $\mu k_m \le 1/4.9$; this maximum value is obtained when $\mu k_e = 1$, and hence corresponds to $k_m = k_e/4.9$.

In addition to selecting a unique, fixed k_m, thereby leading to a phenomenon similar to cell splitting because the flame perimeter continuously expands, the above results raise several remarks. First, one may note that *any* k_e leads to some amplification, in contrast to what would happen if the same noise as in (6.7) was used in the linearized MS equation: as a consequence of (6.12), the condition $\mu k_e<1$ would then have to be met for amplification to occur. The present unconditional amplification is due to the stretch induced by expansion, which makes any disturbance wave number decrease to zero (for seemingly germane situations, see Refs. [35,17]), but here at a final rate that is too low for the Landau-Darrieus instability to be negligible in the limit of long times. Second, the wavelength $2\mu/k_m$ of the most amplified disturbance, as is given by (6.13), depends on both μ (the mixture) and k_e (the noise). Moreover, an *exponential* (as opposed to *algebraic)* growth is predicted, due to the noise which continuously impresses disturbances with a constant wavelength; this growth is faster than all those evidenced by the normal-mode analysis, suggesting that an external noise of approximately fixed wavelength—even if of a weak but fixed amplitude—can ultimately have a strong influence on the flame shape and will soon overcome that due to initially present shape disturbances. Had we considered a noise amplitude which varies only slowly (e.g., algebraically) with time τ, the above conclusion would, of course, not be changed qualitatively; the above argument being linear, consideration of a more broadbanded noise would also lead to an exponential growth. In our opinion this phenomenon may shed a new light on the way experiments could be interpreted when some external noise is acting (i.e., quite often): even the thermal noise could be non-negligible ultimately in actual flames, as well as truncation and roundoff errors in numerical simulations.

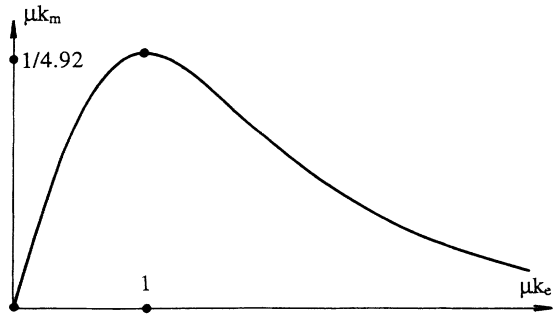

FIG. 5. Reduced wave number μk_m of maximum amplification (see Fig. 4) versus reduced wave number of forcing μk_e.

At the present stage, it is tempting to take a pause and to try comparisons, even if only rough ones, with experiments. With this aim in view, we will consider the classical experiments of [19] on weakly turbulent expanding flames and, more specifically, we first consider the propane air flame slightly rich in fuel shown in picture 8.4 therein, for which the equivalence ratio $r=1.16$ and $u_L\cong 40$ cm/s; if one assumes that the turbulence decay "far from the flame" is not much affected by the large-scale blast flow generated by the flame, the integral and Taylor scales can both be estimated to be close to 0.15 in from the given data on the grid-generated turbulence, from the flame center trajectory, and from the known decay of grid turbulence [36]. We will thus take $2\pi/k_e\cong 0.15$ in. Eyeballing the experimental results reveals that the corresponding front wrinkles are about $\frac{3}{4}$-in to $\frac{2}{3}$-in in wavelength, so that k_m/k_e roughly ranges from $\frac{1}{4}$ to $\frac{1}{5}$; this figure is compatible with the above analysis. We next note that actually (6.13) and (6.14) only depend on the parabolic dependency of the linear growth rate (6.12) pertaining to the planar flame upon the spatial wave numbers; the equality $k\mu=1$ may thus be interpreted as approximately giving the corresponding *actual* marginal wave number. According to the above estimates, 0.15 in (=0.36 cm) should roughly correspond to $k_e\mu\cong 1$, since 4 or 5 are not that far from 4.9. An independent check is provided by *a priori* calculations [37,38] which indicate that the marginal wavelength of the planar problem may be estimated as about $60D_{\rm th}/u_L$ for $\gamma\cong 0.8$ and propane-air flames slightly rich in fuel with a Markstein number of about 4; with $u_L\cong 40$ cm/s and $D_{\rm th}\cong 0.2$ cm^2/s, one obtains 0.33 cm, i.e., a number which is indeed close to $2\pi/k_e=0.36$ cm. Finally, we consider Fig. 7.4 of Ref. [19], which corresponds to about the same flame radius and k_e as above but is associated to a leaner ($r=0.7$) and slower ($u_L\cong 25$ cm/s) flame. Since the Markstein length and the marginal wavelength of lean or not too rich propane-air flames markedly increase as both r and u_L decrease [39], one would reasonably ex-

pect $\mu k_e \geq 1$ for the last experiment; on the basis of (6.13) and (6.14), a larger value of $2\pi/k_m$ than previously and a smaller ratio k_m/k_e should then result. This is compatible with the observed trend. The above reasoning somehow suggests that in moderately turbulent, expanding flames, the mixture properties as well as the large-scale flame geometry and its evolution could all contribute noticeably to the selection of an integral length of wrinkling, besides turbulence itself.

One has to stress, however, that these linear estimates are rather crude and that nonlinear mode-mode interactions may lead to quite different pattern wavelengths from what could be inferred from a linear analysis. The fact that nonlinearity, the subject of the following sections, could play a role even at the visual onset of "spontaneous" instability is quite likely: the first cells which appear experimentally indeed have sharply contrasted polygonlike contours, thereby indicating that noticeable mode-mode couplings are already at work. The above predictions, though encouraging, should thus be considered accordingly.

VII. POLE DECOMPOSITION

We have been unable to solve exactly the fully nonlinear, two-dimensional equation (4.9). The next remark, however, will prove to be useful for our purpose. As

$$\delta(a)(a^2+b^2)^{1/2}\equiv\delta(a)|b| ,$$

writing $\Phi(\tau,\sigma',\sigma'')$ in the form

$$\Phi(\tau,\sigma',\sigma'')=F'(\tau,\sigma')+F''(\tau,\sigma'')+2\mu'\ln(\tau/\tau_0) \tag{7.1}$$

leads to the conclusion that F' and F'' then satisfy the same, one-dimensional equation

$$F_\tau+\frac{1}{2\tau^2}F_\sigma{}^2=\frac{\mu}{\tau^2}F_{\sigma\sigma}+\frac{1}{\tau}I(F,\sigma) . \tag{7.2}$$

Here, σ (F) stands for σ' or σ'' (F' or F'') and the nonlocal operator $I(\ ,\sigma)$ again is the multiplication by $|K|$ in the Fourier space conjugate to σ. Using the above form of Φ, for which (4.9) separates, undoubtedly constitutes a special choice. One has to note, however, that the polar coordinates σ',σ'' which have so far been used are arbitrarily oriented (as is the orientation in a tangent plane to the expanding flame) since no preferred direction exists. As pointed out in [20], cells appearing spontaneously should have the shape of regular curvilinear polygons (triangles, squares, hexagons, etc.) in the absence of symmetry-breaking effects. Though hexagons would certainly be aesthetically preferred, a rectangle is the most general two-dimensional angular domain for which we have so far been able to study Eq. (4.9). For an identical shape of the integration domain, a comparison between analytical and numerical results [1] reveals that a separation of variables similar to (7.1) gives meaningful solutions for the MS equation. One has also to recall that the orthogonal patterns implied by (7.1) are not that different from what is *locally* observed in reality (e.g., see [20], Fig. 5)—hence, our choice. We next note that no reason exists why σ' and σ'' should play different roles when the most general initial conditions compatible with (7.1) are used; it is then sensible to further assume

$$F'(\tau,\ )=F''(\tau,\ )=F(\tau,\ ) . \tag{7.3}$$

Along the same lines, it is reasonable to study (4.9) over a square and with periodic boundary conditions, because the spherical patch corresponding to $O(1)$ values of σ' and σ'' is completely anonymous and what happens along its boundary should be as independent as possible on directions and arclengths.

In addition to being one dimensional, and hence presumably simpler to study than (4.9), Eq. (7.2) has the further pleasant property that exact solutions which are $2\pi/K$ periodic in σ can be written in terms of known functions. They correspond to

$$F_\sigma(\tau,\sigma)=-\mu K\sum_{\alpha=1}^{2N}\cot\left[\frac{K}{2}[\sigma-\sigma_\alpha(\tau)]\right] . \tag{7.4}$$

The σ_α's can be identified with the poles of F_σ in the complex σ plane, and they ought to appear in conjugate pairs in (7.4) for $F(\tau,\sigma)$ to be real when σ is. In addition, in order that (7.2) be satisfied, the σ_α's must evolve according to coupled, ordinary differential equations ($\alpha=1,\ldots,2N$):

$$\dot\sigma_\alpha=\frac{\mu K}{\tau^2}\sum_{\beta\neq\alpha}\cot\left[\frac{K}{2}(\sigma_\beta-\sigma_\alpha)\right]-\frac{i}{\tau}\,\mathrm{sgn}[\mathrm{Im}(\sigma_\alpha)] , \tag{7.5}$$

where $\dot\sigma_\alpha\equiv d\sigma_\alpha/d\tau$ and $\mathrm{Im}(\sigma_\alpha)$ stands for the imaginary part of σ_α. The above equations are readily demonstrated by adapting the results obtained by Lee and Chen [26] for models of plasma instabilities, or those obtained by Thual, Frisch, and Henon [27] for the MS equation (1.1) itself, to the present situation (Renardy [40] and Minaev [41] independently obtained particular cases by alternative methods). This basically requires first noting that the terms which involve $F_\sigma{}^2$ and $F_{\sigma\sigma}$ have the same explicit dependence on time (here, $1/\tau^2$), so that their most divergent contributions in each cell (in the complex σ plane) again automatically cancel one another, in much the same way as they did in the MS equation. In physical terms this corresponds to the fact that curvature is able to smooth out the sharp crests that are invariably generated by a Huygens-like propagation. Next, one may remember the functional equation (a mere trigonometric identity) fulfilled by cot( ), viz.,

$$f(a)f(b)+1+f(a-b)[f(a)-f(b)]=0 , \quad a\neq b . \tag{7.6}$$

Using it with $a=K(\sigma-\sigma_\alpha)/2$ and $b=K(\sigma-\sigma_\beta)/2$, ($\alpha\neq\beta$) indeed allows one to transform the remaining nondiagonal terms obtained when plugging (7.4) into $F_\sigma{}^2$. The final step is to note that, when applied to $\cot[K(\sigma-\sigma_\alpha)/2]$, the nonlocal operator appearing in (7.2) is about the same as a differentiation, apart from a multiplicative coefficient ($\pm i$) that depends on the sign of $\mathrm{Im}(\sigma_\alpha)$ and from an additive constant: this is so because

the Fourier transform of $\cot[K(\sigma-\sigma_\alpha)/2]$ has a one-sided support. As for the additive constant, it is akin to an effect which is very familiar to fluid mechanicists: whereas a simple line source of fluid yields a flowfield which decays radially to zero, a linear array of sources produces a stream at infinity.

Once the total number ($2N$) and the initial locations $[\sigma_\alpha(\tau_0)]$ of the poles are specified at some positive initial time (τ_0), and if values are assigned to the "Markstein constant" μ and to the harmonic number K, the pole trajectories are fully determined, thereby in principle allowing one to compute the evolutions in flame shape via an integration of (7.5). The mean flame speed variations $\langle -\Phi_\tau \rangle$ can be computed upon averaging (7.2) with respect to the angular variables. This gives

$$\langle -\Phi_\tau \rangle = -\frac{2\mu'}{\tau} + \frac{1}{\tau^2}\langle F_\sigma{}^2 \rangle \ , \tag{7.7}$$

since the solutions are periodic in σ' and σ'' and because we assume that σ' and σ'' play identical roles; if the flame shape disturbance were to depend only on σ' (or σ''), the contribution of $F_\sigma{}^2$ to (7.7) should be halved. Equation (7.7) clearly displays two distinct, possibly antagonistic influences on the mean flame speed: a mean curvature effect, the sign of which is fixed by μ', and the increase in flame area induced by the instability.

Using (7.4) into (7.7), one may next show that

$$\langle -\Phi_\tau \rangle = -\frac{2\mu'}{\tau} + \frac{4\mu NK}{\tau}\left[1-\frac{\mu NK}{\tau}+\frac{\tau}{N}\sum_{\alpha=1}^{N}\dot{B}_\alpha\right] , \tag{7.8}$$

where the positive, real numbers $B_\alpha(\tau)$ are the imaginary parts of the poles of F_σ that are located in the upper half-complex plane. When applied to the MS equation itself, the algebra leading to (7.8) also works for any pole-decomposable solution to (1.1) and yields a "nearly planar" analog to (7.8), viz.,

$$\langle -\phi_\tau \rangle = 2\mu kN\left[1-\mu kN+\frac{1}{N}\sum_{\alpha=1}^{N}\dot{b}_\alpha\right] , \tag{7.9}$$

where $2\pi/k$ is the (spatial) period and the b_α's refer to the poles of ϕ_X; beside illustrating the differences between the nearly planar and the nearly spherical configurations, the above result generalizes a formula previously obtained in particular case [28] and is fully compatible with the infinitely many bifurcations evidenced by Renardy [40] concerning the steady MS equation. At any rate, Eq. (7.8) is convenient for computing $\langle -\Phi_\tau \rangle$ in terms of a minimum number of currently available quantities while numerically determining the pole trajectories.

In addition to appearing—with the $1/\tau$ factors suppressed—in the context of the MS equation [27], equations similar to (7.5) have recently been shown to control the evolution of wrinkles of finite amplitude superimposed to a nearly parabolic steady flame [17]. The main difference between the latter case and the present one was the replacement of $1/\tau$ in (7.2) and (7.5) by the rapidly decreasing function of time: $e^{-S\tau}$, $S>0$. The functional difference between the two cases reflects the different ways in which the wrinkles are stretched. The analogy between (7.2) and the governing equation for nearly parabolic, steadily propagating flames is best displayed if one again introduces the arclength $X=\sigma\tau$ and the notation $\phi(X,\tau)=F(X/\tau,\tau)$. This transforms (7.2) into

$$\phi_\tau+\frac{1}{\tau}X\phi_X+\tfrac{1}{2}\phi_X{}^2=\mu\phi_{XX}+I(\phi,X) \ . \tag{7.10}$$

In the case of nearly parabolic flames, the pseudoconvective term $X\phi_X$ had the time-independent trough curvature $S>0$ as a factor, in lieu of $1/\tau$.

VIII. EXAMPLE OF NONLINEAR FLAME DYNAMICS: $N=1$

To begin with, we consider the simplest situation, in which only two poles $A\pm iB$ are involved in each sector of $2\pi/K$ angular extent; B may be assumed positive, without loss of generality. Equations (7.4) and (7.5) then give $\dot{A}=0$, so that the disturbance stays *angularly fixed,* and

$$F_\sigma = -2\mu K \sin[K(\sigma-A)]/\{\cosh(KB)-\cos[K(\sigma-A)]\} \ , \tag{8.1}$$

$$\dot{B}=\frac{\mu K}{\tau^2}\coth(KB)-\frac{1}{\tau} \ . \tag{8.2}$$

At early times ($\tau\ll 1$) the first term in the right hand side of (8.2) clearly dominates, since $\coth(KB)>1$. Therefore, $\dot{B}>0$ for $\tau\ll 1$ and the disturbance amplitude first decays, in accord with the linear initial value analysis of Sec. VI; the Landau-Darrieus instability, which gives the last term in (8.2), only plays a secondary role during this early period of time, and the dynamics is then Burgers like. We next consider the situations in which $0<KB\ll 1$ and τ is finite; because $\dot{B}$ is again positive [$\coth(KB)\sim 1/KB\gg 1$], B cannot vanish when τ is finite. Lastly, we tentatively assume that B may remain different from zero even for $\tau=\infty$; if true, this assumption would imply $B(\tau\gg 1)=-\ln\tau+\text{const}$ by Eq. (8.2), thereby leading to a contradiction since B would have vanished at least once. The only remaining possibility is thus $B(\tau<\infty)>0$, $B(\infty)=0$. From (8.2) one then deduces

$$B(\tau\to\infty)=\mu K/\tau+O(1/\tau^2) \ . \tag{8.3}$$

By contrast to what happened to the periodic, two-pole disturbances of parabolic flames [17], for which the $1/\tau$ factors in (8.2) were replaced by the *integrable* function $e^{-S\tau}$ ($S>0$), the present, geometry-induced time-dependent stretch has a final rate that is too low to prevent B from going to zero. Equation (8.3) is valid whatever the values assigned to μ, K, $B(\tau_0)$, and τ_0. The above conclusion about $B(\tau)$ can be reformulated in terms of the reduced, peak-to-peak amplitude $\Gamma(\tau)$, defined by

$$2\Gamma(\tau)=F_{\max}(\tau)-F_{\min}(\tau)$$

and satisfying

$$\Gamma(\tau)=2\mu\ln\{\coth[KB(\tau)/2]\}\ . \tag{8.4}$$

According to (8.3), $\Gamma(\tau)$ always diverges as $\tau\to\infty$, though mildly: $\Gamma(\tau\to\infty)=O(\ln\tau)$. That $\Gamma(\tau)$ and the instantaneous wavelength $2\pi\tau/K$ ultimately evolve in logarithmic proportions can be related back to the following two properties.

(i) $B(\tau)\to 0$ implies that each pole of F_σ ultimately mainly interacts with its complex conjugate in its own cell (rather than with its images and their conjugates in neighboring cells), and the solution locally approaches the nonperiodic, two-pole elementary crest.

(ii) The latter *non*periodic, two-pole solution to (7.2) has an amplitude $F(\sigma,\tau)$ which diverges logarithmically with real distance from the poles [27]. The basic reason is that the Green's function of the two-dimensional Laplace's equation is a logarithm.

Although the absolute amplitude $\Gamma(\tau)$ diverges (Fig. 6), the *relative* amplitude $C(\tau)=\Gamma(\tau)/\tau$ ultimately decays to zero, though at a very slow pace: $C(\tau)\sim\tau^{-1}\ln\tau$ (see Fig. 7). The above findings are in qualitative agreement with what is observed in reality [19,20]—at least during the "not-too-late" evolutions of "spherical" flames in quiescent gases: the sharp flame shape disturbances that are presumably created initially by the electrodes soon form ridges or "cracks" which approximately stay at fixed angular locations while their relative amplitude slowly decreases to zero. These results, however, *contradict* those of the linear analysis of the initial value problem given in Sec. VI A, because $C(\tau)$ is now predicted to decay to zero whatever the values assigned to μ, K, τ_0, and $C(\tau_0)$. Of course, it could be argued that a two-pole solution has nothing to do with the one-mode disturbances of infinitesimal amplitudes which we considered in Sec. VI A; this is not true. Indeed, integrating (8.1) yields

$$F(\tau,\sigma)=h(\tau)-2\mu\ln[1-\cos K(\sigma-A)\,\mathrm{sech}\,KB]\ , \tag{8.5}$$

where the magnitude of the "constant" of integration $h(\tau)$ is determined by $h_\tau\sim\langle F_\sigma{}^2\rangle$. For $KB\gg 1$, the above expression leads to

$$F(\tau,\sigma)=4\mu e^{-KB}\cos K(\sigma-A)+\cdots\ . \tag{8.6}$$

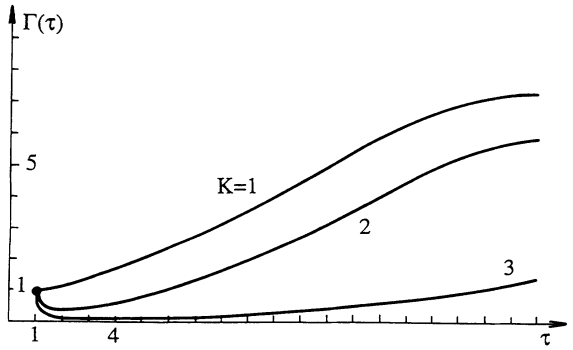

FIG. 6. Peak-to-peak amplitude $\Gamma(\tau)$ of a two-pole-per-cell solution to Eq. (7.2), for $\tau_0=1$, $\Gamma(\tau_0)=1$, and different K's.

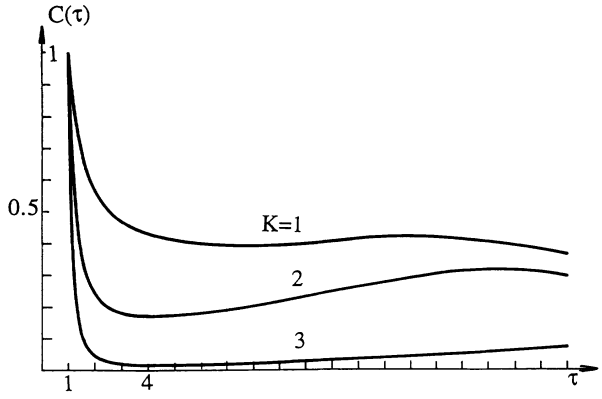

FIG. 7. Relative amplitudes $C(\tau)=\Gamma(\tau)/\tau$ corresponding to Fig. 6.

Given (8.4), this is nothing but (6.1), so that the pole decompositions play the role of nonlinear Fourier transformations. In our opinion, the typically nonlinear effect leading to the results plotted in Fig. 8 and to the difference with Fig. 2 may well be one of the reasons linear analyses of the initial value problem underestimate the flame radius at the "visual" onset of instability, consistent with the remark made by Zel'dovich *et al.* [5], about this point, because the (early) growth of C is slower than expected, due to the *stabilizing* nonlinear effects. A small departure from sphericity [$C(\tau)\ll 1$] does not imply that the assumption of a small amplitude is applicable [$\Gamma(\tau)\gg 1$]. Figure 8 also suggests that a frequently used argument [5,23], according to which the onset of instability should actually be defined as the time when $C(\tau)$ resumes its initial value $C(\tau_0)$, instead of τ_*, is somewhat artificial: in some cases, $C(\tau)$ always stays below $C(\tau_0)$. One must nevertheless acknowledge that using only two poles may lead to a quite peculiar solution, and that more general disturbances should be considered.

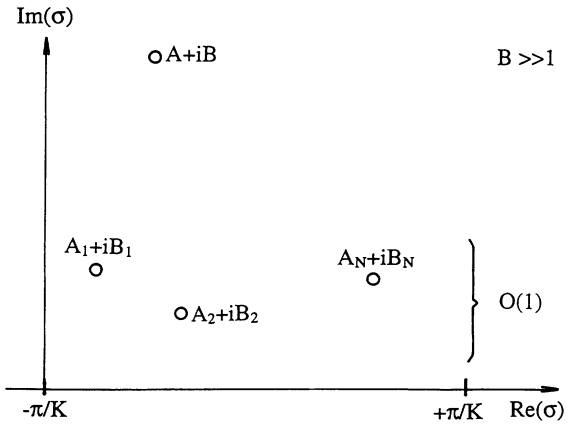

FIG. 8. Initial pole locations (only the upper half of a complex cell is shown) corresponding to the $(2N+2)$-pole situation.

IX. NEXT EXAMPLE: $2N+2$ POLES

We now consider situations in which the "unperturbed" background flame shape is no longer perfectly spherical initially but already includes the wrinkles of finite amplitudes due to $2N$ preexisting poles $A_\alpha \pm iB_\alpha$ [$\alpha=1,\ldots N$; $KB_\alpha \leq 0(1)$; $B_\alpha>0$]. An extra pair $A\pm iB$, with $B>0$ and $KB \gg 1$, is also involved and represents an extra wrinkle of small amplitude (Fig. 8). Using (7.5), and the fact that

$$0<\tanh[K(B\pm B_\alpha)]\cong 1$$

for any α, one deduces an approximate equation for $B(\tau)$:

$$\dot{B}\cong(2N+1)K\mu/\tau^2-1/\tau\ , \tag{9.1}$$

which may be used whatever the phases A_α and A. As is shown by comparing (9.1) to (8.2), the preexisting disturbance(s) tend(s) to delay the growth of the extra wrinkle, as a consequence of *nonlinear* pole-pole interactions. Though small, the contribution of the substructure to the flame shape is not directly amenable to the linear analysis reported in Sec. IV A; in more physical terms, one could say that the preexisting extra curvature modifies the way in which a new wrinkle evolves. A comparison of (9.1) to the large-B limit of (8.2) readily shows that the relative amplitude corresponding to (9.1) follows an equation similar to (6.4), but with μ replaced by $(2N+1)\mu$. The analog of $\dot{C}=0$ is now obtained when

$$\tau=(2N+1)\mu K^2/(K-1)\ ,$$

instead of (6.6), and the onset of (secondary) instability corresponds to $\tau_*=4\mu(2N+1)$, instead of $\tau_*=4\mu,\ldots$ according to Istratov and Librovich's criterion. Because the above result is independent of the phases $A_1,\ldots,A_N$, it indicates that angularly localized initial disturbances, such as those impressed by electrodes, may shift the onset of small-scale instability to larger flame sizes than what is predicted by (6.4). This holds even if the preexisting disturbances of finite amplitude only have a small relative amplitude: it suffices to consider the case of $N=1$, for example, which leads to $\Gamma(\tau)/\tau\sim\ln\tau/\tau\ll 1$ in the long time limit but nevertheless yields $2N+1=3$, and hence triples the effective τ_*.

As long as $KB\gg 1$, one may integrate (9.1) into

$$KB=KB(\tau_0)-\ln(\tau/\tau_0)^K+\mu K^2(2N+1)(1/\tau_0-1/\tau)\ . \tag{9.2}$$

For the extra wrinkle to acquire a noticeable amplitude [corresponding to $KB=0(1)$, say], one must wait until

$$(\tau/\tau_0)>O\left[\exp\left[B(\tau_0)+\frac{\mu K}{\tau_0}(2N+1)\right]\right]\ , \tag{9.3}$$

i.e., $\tau\gg\tau_0$ even if $B(\tau_0)$ and N are only moderately large. As a by-product, (9.3) also suggests that strong, localized initial disturbances ($N\to\infty$) may well be linearly stable. To summarize, one may say that preexisting disturbances inhibit the growth of extra ones so strongly that the help of external forcing is likely to be needed if everlasting cell splitting is to be obtained.

X. PETAL-LIKE PATTERNS AND THEIR STABILITY

In the limit of long wavelengths, the physically relevant steady solutions to the MS equation (1.1) acquire a shape which is independent of scales and have a peak-to-peak amplitude of wrinkling that increases *proportionally to the wavelength* itself, by contrast to the two-pole periodic solutions for which the amplitude only grows *logarithmically*. The corresponding scale-independent shape can be computed numerically from a truncated MS equation [42] in which curvature effects are neglected; alternatively, it can be obtained analytically [27] for it formally corresponds to a steady continuous distribution of poles that are aligned along a parallel to the imaginary X axis in each complex cell.

Guided by the analogy with the planar case and because the wavelength of wrinkled expanding flames grows linearly with time, one is naturally led to seek solutions to the "spherical" MS equation (7.2) in the following form:

$$F(\tau,\sigma)=\tau F_0(\sigma)+o(\tau)\ ,\quad \tau\to\infty\ . \tag{10.1}$$

These correspond to asymptotically self-similar, "petal-like" cells (Fig. 9) whose absolute amplitude is *proportional to* τ, by contrast to the corresponding two-pole solution (8.1) for which the *logarithmic* growth $\Gamma(\tau)\sim\ln\tau$ was obtained. For $\tau\to\infty$, substitution of (10.1) into (7.2) gives the truncated equation

$$F_0+\tfrac{1}{2}(F_{0\sigma})^2=I(F_0,\sigma)\ , \tag{10.2}$$

which holds far from the crests. When integrated over an angular sector $[-\pi/K,\pi/K]$ with periodic conditions on F_0, (10.2) yields wrinkled shapes that depend on K; for $K\to\infty$, $F_0\sim 1/K$ and F_0 tends to the solution pertaining to the "planar" case, up to dilations. We did not attempt to accurately describe $F_0(\sigma;K)$ in detail, because it is enough for our purpose to note that the following behavior:

$$F_{0\sigma}(\sigma;K)=s(K)\sigma+O(\sigma^3)\ ,\quad s(K)>0\ ,\ s(0)=0\ , \tag{10.3}$$

holds close to a trough (located at $\sigma=0$, without loss of

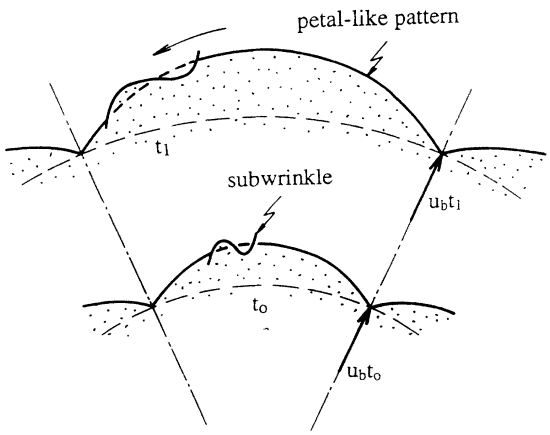

FIG. 9. Asymptotically self-similar, "petal-like" pattern, Eq. (10.1), and secondary wrinkles.

generality).

To study the stability of these petal-like solutions, we proceed in the same way as we did [17] for nearly parabolic flames—namely, the general solution to (7.2) is written as

$$\tau F_0(\sigma,\tau)+f(\sigma,\tau)+\cdots ,$$

where F_0 is given by (10.1) and f represents subwrinkles of smaller scale for which curvature effects may be nonnegligible. For large values of τ, the evolution of f close to the *(wider and wider)* troughs of the basic solution (10.1) is then approximately governed by

$$f_\tau+\frac{1}{2\tau^2}f_\sigma{}^2+\frac{s}{\tau}\sigma f_\sigma=\frac{\mu}{\tau^2}f_{\sigma\sigma}+\frac{1}{\tau}I(f,\sigma) , \quad (10.4)$$

because $F_\sigma\sim\tau\sigma s(K)$ locally. Once linearized, (10.4) is readily solved to give the elementary particular solutions

$$f=g(\tau)\exp[i\kappa(\tau)\sigma] , \quad (10.5)$$

with

$$\kappa(\tau)=\kappa(\tau_0)(\tau_0/\tau)^s \quad (\kappa_0,\tau_0>0) , \quad (10.6)$$

$$g(\tau)=g(\tau_0)\exp\left[\int_{\tau_0}^{\tau}\frac{\kappa(u)}{u}\left[1-\mu\frac{\kappa(u)}{u}\right]du\right] . \quad (10.7)$$

Two results worth noting can be gained from (10.6) and (10.7). The first is that the subwrinkles have an instantaneous wave number $\kappa(\tau)/\tau$ which decays to zero faster than $1/\tau$, whatever the exact value of the additional rate of tangential strain ($s>0$) induced by the curvature of F_0. For the same reason, the substructure amplitude saturates as $\tau\to\infty$; this is perfectly compatible with (9.3), because the self-similar cells formally correspond to $N=\infty$. In other words, the petal-like patterns are *linearly stable,* unlike the expanding spherical flame. The final amplitude $\mu g(\infty)$, readily computed from (10.7), is maximum if the initial disturbance wave number $\kappa(\tau_0)/\tau_0$ satisfies $\mu\kappa_0/\tau_0=1+1/(2s)$; $g(\infty)$ then reads

$$g(\infty)=g(\tau_0)\exp[\tau_0(1+2s)/4\mu s^2] . \quad (10.8)$$

Consequently, the amplitude will remain small [$g(\infty)<O(\mu)$, say] if $g(\tau_0)$ meets the condition

$$g(\tau_0)<O(g_c) , \quad g_c\equiv\mu\exp[-\tau_0(1+2s)/4\mu s^2] . \quad (10.9)$$

Though linearly stable, the self-similar pattern becomes more and more sensitive to disturbances as time elapses; even the ever present thermal noise (as well as roundoff errors in numerical experiments) would ultimately trigger the appearance of substructures in expanding flames.

One can next see what happens if $g(\tau_0)$ markedly exceeds g_c. In a sense, (10.4) is in effect a local restriction of (7.2) and, as such, it can also certainly be solved by the pole-decomposition method. Writing $f_\sigma(\tau,\sigma)$ in the form

$$f_\sigma=-\mu\kappa_0\sum_{\alpha=1}^{2n}\cot\left[\frac{\kappa_0}{2}(c-c_\alpha)\right] (\kappa_0>0,\ n\ \text{integer}) , \quad (10.10)$$

with $c\equiv\sigma/\tau^s=X/\tau^{s+1}$ and $c_\alpha=a_\alpha+ib_\alpha$, indeed results in equations similar to (7.5) for the complex poles c_α of f_σ, the only, but crucial, structural difference with (7.5) consists of the replacement of $1/\tau$ by $1/\tau^{s+1}$. For example, the simplest periodic subwrinkle ($n=1$, $c_1=a+ib$, $c_2=a-ib$, $b>0$) has its dynamics governed by $a=0$ and [compared to (8.2)] by

$$\dot b=\frac{\mu\kappa_0}{\tau^{2+2s}}\coth(\kappa_0 b)-\frac{1}{\tau^{s+1}} . \quad (10.11)$$

Because $1/\tau^{s+1}$ is integrable at $\tau=\infty$ (like $e^{-s\tau}$ but unlike $1/\tau$), $b(\infty)$ may remain bounded away from zero if $b(\tau_0)$ is large enough (small initial amplitude), consistent with (9.1); alternatively, $b(\tau)$ decays to zero like $1/\tau^{1+s}$ if $b(\tau_0)$ is less than a critical value $b_c(\tau_0,\kappa_0,\mu,s)$. When the latter condition—a nonlinear analog of (10.9)—is met, the amplitude $g(\tau)$ grows limitlessly with τ, because

$$g(\tau)=2\mu\ln\coth[\kappa_0 b(\tau)/2] .$$

The above results suggest that the petal-like cells of a steadily expanding flame are *metastable* at the most, the critical amplitude $\sim g_c(\tau_0)$ of disturbance needed to trigger the growth of extra substructures of finite amplitude being an *exponentially decreasing* function of time τ_0 at which those extra disturbances are imprinted. Of course, the petals with wider troughs ($K\ll 1$, and hence $0<s\ll 1$) are especially vulnerable. To conclude this section, it is again suggested that *some* noise is needed to induce cell splitting and that *any* noise will ultimately have an important influence.

XI. GENERAL 2N-POLE DYNAMICS

When many interacting pairs of poles are involved in each cell, several mechanisms are simultaneously at work—namely, the Landau-Darrieus instability, which tends to push each pair of poles against the real axis and, therefore, to produce real logarithmic singularities in $F(\tau,\sigma)$, i.e., spikes pointing towards the burned gases; the interaction between complex conjugate pairs, which suppresses the aforementioned singularities (see the two-pole solutions), and smooths out the front crests; the wavelength stretch induced by expansion, which tends to make each crest move apart from its neighbors; and the tendency of poles to form alignments along the imaginary σ axis, which tends to reinforce the biggest wrinkles.

The last effect was first evidenced by Thual, Frisch, and Henon [27]. It explains why the MS equation leads generically to a single steady fold with the maximum available wavelength, and is also a consequence of the pole-pole interactions, i.e., of nonlinearity (it is the focusing effect due to $F_\sigma{}^2$, which exists even in the inviscid Burgers equation). It also acts in the present case. Indeed, when two poles $\sigma_\alpha,\sigma_\beta$ are momentarily very close to each other in the upper σ plane, Eq. (7.5) leads to

$$\dot\sigma_\alpha\cong\frac{2\mu}{\tau^2}\frac{1}{\sigma_\beta-\sigma_\alpha}+j(\tau) , \quad \dot\sigma_\beta\cong\frac{2\mu}{\tau^2}\frac{1}{\sigma_\alpha-\sigma_\beta}+j(\tau) , \quad (11.1)$$

where $j(\tau)$ is common to σ_α and σ_β, and results from interactions with the other poles. From (11.1) one has

$$(\sigma_\alpha-\sigma_\beta)^2\cong 8\mu(1/\tau-1/\tau_0)+\varepsilon\ , \tag{11.2}$$

where ε is a small complex constant [the value of $(\sigma_\alpha-\sigma_\beta)^2$ at $\tau=\tau_0$]. When τ is not large, σ_α and σ_β remain close to each other during a short period of time (a collision at $\tau\cong\tau_0$, in a sense) so that one may then write

$$(\sigma_\alpha-\sigma_\beta)^2\cong-\frac{8\mu}{\tau_0^2}(\tau-\tau_0)+\varepsilon\ . \tag{11.3}$$

In the same way as in the case of the MS equation, the two poles tend to attract each other in a direction parallel to the real σ axis and repel each other along the imaginary axis (Fig. 10); given the structure of (11.3), this occurs faster when τ_0 is small. The mechanism certainly tends to build the aforementined pole alignments again (now in the σ plane), and to reinforce the sharpest, preexisting disturbances. When τ is large, however, the approximation leading from (11.2) to (11.3) fails. Though very efficient at early times, the above mechanism is headed to be quenched in the long time limit, since $1/\tau$ goes to zero in Eq. (11.2). This is so because the tendency to form vertical alignments *in the σ plane* is counteracted by the flame expansion, which tends to make the disturbances move away from each other *in the X plane* ($X\equiv\sigma\tau$); this can be seen by writing $X_i=\tau\sigma_i$ ($i=\alpha,\beta$), which transform (11.1) into

$$\frac{d}{d\tau}(X_\alpha-X_\beta)^2=-8\mu+\frac{2}{\tau}(X_\alpha-X_\beta)^2\ . \tag{11.4}$$

Ultimately this leads to $(X_\alpha-X_\beta)^2\sim\tau^2$ and hence to angularly separated crests.

The overall outcome of these $2N$-body interactions is rather difficult to predict analytically in the general case and, so in order to have more information, we integrated (7.5) numerically. In the absence of any specific information, we used an irregular initial condition on F. To construct a $2\pi/K$-periodic, noiselike initial condition of small amplitude $F(\tau_0,\sigma)$ which is pole decomposable and has an almost flat, angular energy spectrum for all harmonic numbers less than $(M+1)|K|$ in absolute value, one may consider

$$F(\tau_0,\sigma)=-2\mu\sum_{n=1}^{M}\ln\{1-\operatorname{sech}(KB)\cos[nK(\sigma-A_n)]\}\ , \tag{11.5}$$

where $K>0$, $B>0$, and the A_n's are samples at random uniformly over $[0,2\pi]$. If $KB\gg1$ and σ is real, (8.6) indicates that

$$F(\tau_0,\sigma)=4\mu e^{-KB}\left\{\sum_{n=1}^{M}\cos[nK(\sigma-A_n)]+O(e^{-KB})\right\}\ . \tag{11.6}$$

On the other hand, (11.5) corresponds to M linear rows of poles (plus their complex conjugates) which are aligned along M parallels to the real σ axis. Specifically, the nth pair of rows contains poles that are located (Fig. 11) at

$$\sigma=A_n+\frac{2\pi}{|K|}\frac{m}{n}\pm i\frac{B}{n}\ ,\quad m=1,2,\ldots\ ,\quad (\mathrm{mod}\,n)\ . \tag{11.7}$$

Using an n-dependent value of B in (11.5) would allow one to mimic any initial spectrum over the range $[-M|K|,M|K|]$ of angular harmonics.

The pole equations (7.5), endowed with (11.5) as initial condition, were integrated by a numerical routine (fourth-order Runge-Kutta, variable step size). Typically, $\mu=1$ and $M=10$ [hence, $2N=M(M+1)=110$] were employed. We took $\tau_0=1$, i.e., is less than the time of "instability onset" corresponding to the Istratov-Librovich criterion. We chose $K=1$ because this gives twice the angular sector corresponding to the "most dangerous" mode $K_*=2$ which the normal-mode analysis singled out in Sec. VI A. As for KB, we adopted $KB=5$, so that $e^{-KB}\cong\frac{1}{150}$ is indeed small. The relative amplitude $C(\tau)$ is now defined as $2\tau C(\tau)=F_{\max}-F_{\min}$. A dynamics imitating a repeated cell splitting would manifest itself by a regular "rain" of poles towards the real axis, in such a way that the mean spacing between front crests would be approximately constant in time.

Figures 12 and 13 show a few typical consecutive

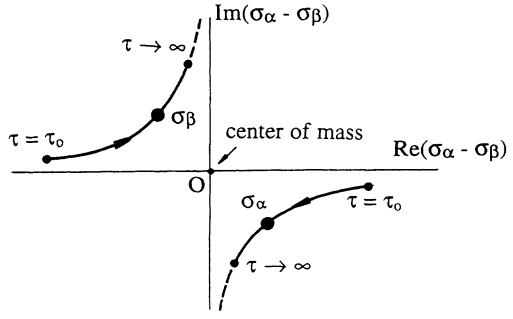

FIG. 10. Near collision of two poles $\sigma_\alpha,\sigma_\beta$ as seen from their "center of mass," Eq. (11.2).

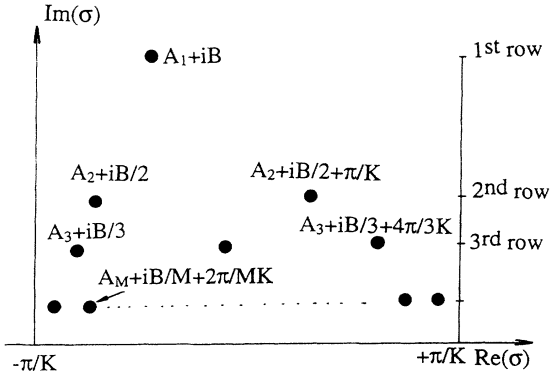

FIG. 11. Pole locations (only the upper half of a complex cell is shown) corresponding to the irregular, M-row initial condition [Eqs. (11.5) and (11.6)]; the phases $A_1,\ldots,A_M$ were sampled at random uniformly on $[0,2\pi/K]$.

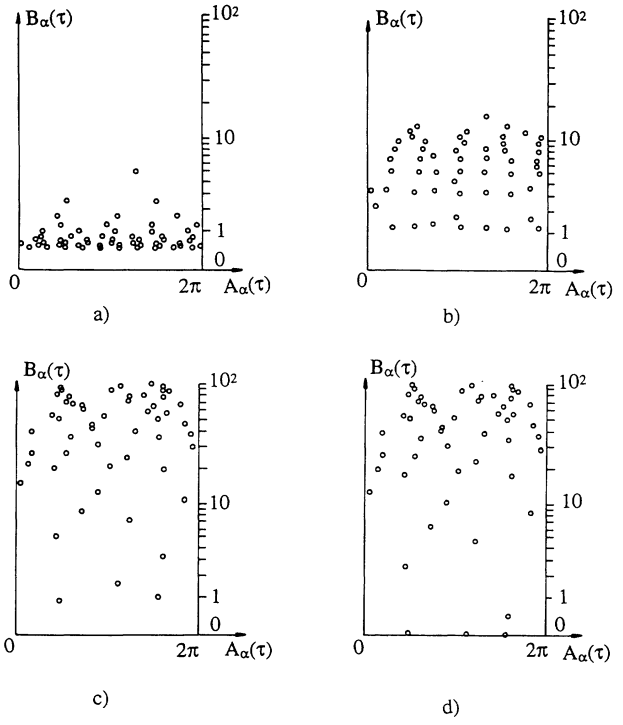

FIG. 12. Successive snapshots of the pole population obtained from integration of Eq. (7.5) with $\tau_0=\mu=K=1$, $M=10$; only the upper-half of a complex cell is shown. (a) $\tau=\tau_0=1$, (b) $\tau=1.111$, (c) $\tau=30$, and (d) $\tau=650$.

snapshots of the pole population. Very quickly, all the imaginary parts $B_\alpha(\tau)$ increase, so that $C(\tau)$ decays; meanwhile, the poles tend to aggregate in chainlike structures parallel to the imaginary axis, in accord with what (11.1) indicates. Then comes a time $\tau\cong 4=\tau_*$ at which time the smallest B starts decreasing, but one has to wait until $\tau\cong 8$ before $C(\tau)$ reaches a minimum and until $\tau\cong 20$ for it to acquire a value comparable to $C(1)$. Only when $\tau\cong 100$ does the front display sharp crests and wide troughs; $\tau\cong 100$ also corresponds to $C(\tau)$ reaching its

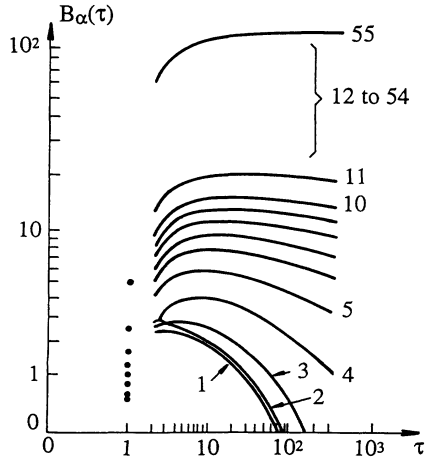

FIG. 13. Trajectories of the pole imaginary parts $B_\alpha(\tau)$ ($\alpha=1,\ldots,55$) in upper-half σ plane (same conditions as in Fig. 12).

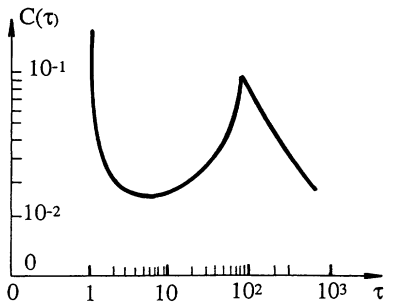

FIG. 14. Relative amplitude of wrinkling $C(\tau)$ vs time τ (same conditions as in Figs. 12 and 13).

maximum, Fig. 14. As for the more remote poles, they qualitatively behave as predicted in Sec. IX: the larger their imaginary part, the slower the poles approach the real axis. Even for very long times ($\tau<100$), only three to four (pairs of) poles effectively acquire $O(1)$ imaginary parts; halving K, i.e., effectively doubling the front arc-length, merely doubles the number of poles that ultimately participate to the flame shape for $\tau<100$, hence the number of crests belonging to the "first generation" of mature crests. Increasing the number of rows to $M=25$ did not seem to change the conclusion. The above results are very preliminary and more systematic studies should be undertaken, but they do suggest that no tendency to repeated cell splitting spontaneously occurs over the periods of time which we considered, even though those noticeable exceed the time $\tau_*=4\mu$ selected by a normal-mode analysis and the criterion proposed in [22]. Instead, a single "generation" of wrinkles is obtained for $\tau\leq O(25\tau_*)$ and its very appearance strongly delays the buildup of extra crests.

XII. CONCLUDING REMARKS

In the conclusion to their work [19], Palm-Leis and Strehlow wrote that "... our understanding of the propagation of transient curved flames is incomplete at the present time. Further work on both transient and steady curved flames, as well as on inherent and driven instabilities, is needed before a quantitative understanding of even the simplest turbulent flames may be obtained." Despite the numerous theoretical or experimental works which have been devoted to the subject since that time, one may reasonably acknowledge the fact that the above statements are still partly true. It is our hope that the present analyses contribute to filling the gap.

A time-dependent generalization (4.9) of the MS equation was derived as a tool to study the dynamics of nearly spherical, expanding wrinkled flames. In the linear domain it basically reproduces what classical analyses gave as result: ultimate algebraic growth of each angular mode of infinitesimal amplitude; existence of a particular mode, the relative amplitude of which has the shortest time of decay τ_*; and equality between τ_* and the reciprocal maximum growth rate of perturbations of nearly planar fronts. Our evolution equation has a further ad-

vantage in that it gives access to the dynamics of wrinkles of finite amplitudes through a $2N$-body problem for the complex singularities of the flame front shape, thereby allowing a few specific effects of nonlinearity to be evidenced: ultimate logarithmic growth of elementary crests, metastability of self-similar patterns, quenching of the crest coalescence process by expansion, and existence of a first generation of sharp wrinkles appearing noticeably later than τ_* (typically at $\tau \cong 25\tau_*$). All these nonlinearity-related trends qualitatively suggest why a linear analysis notably underestimates the time of visual onset of instability in expanding flames, and are compatible with the experiments, for "not-too-late" evolutions.

However, we cannot ignore one disappointing conclusion: the pole-decomposable solutions (7.4) to (7.2) in the form in which we have exploited them so far, did not account for the *endless* phenomenon of cell splitting which is often experimentally observed [20,34] as flames keep on expanding. In a sense, this is a perfectly logical result in the framework of (7.1) and (7.2) because, when finite, the total number ($2N$) of involved poles is a *constant of motion* for (7.2): therefore, the maximum number (N) of isolated ridges that they can produce is clearly too small to evenly cover the surface of an ever growing flame with wrinkles of constant average wavelength. Even worse, no obvious trend of transient cell splitting showed up during the preliminary numerical runs reported in Sec. XI. If one still believes that (4.9) is a model equation qualitatively suitable for use as a starting point (as supported by the work of [47]), one can conceive a few hypotheses (1)–(4), which we briefly examine below, about the origin of this deficiency and ways of understanding it.

(1) The pole-decomposable solutions to (7.2) could be a class that is too restricted and accordingly cannot imitate the flame behavior as $\tau \to \infty$, that is, when the front gets locally planar. Though this is a possibility which seems plausible, the following remarks are due: Except if F always has to be an entire function (but this cannot be true, as pole-decomposable, exact solutions can be used initially), $F_\sigma(\tau,\sigma)$ must diverge at singularities of some kind in the complex σ plane; otherwise, it would be a *constant*, according to Liouville's theorem on bounded analytic function [43]. Given the form of (7.2), we found it difficult to imagine a different locally dominant balance of its mostly divergent terms from that leading to movable simple poles with the same residue ($=-2\mu$); in addition, if analytic and bounded, the difference between F_σ and its pole-decomposed form would also be a constant; again due to Liouville's theorem. The pole-decomposable solutions thus seem to be quite viable ones, except if the *general* solution to the evolution equation always possesses an entire component when the initial profile is not pole decomposed. The last remarks point out the very difficult problem of pole "creation" from an entire initial function [e.g., $F=\sin(K\sigma)$] or from an initial condition such that F_σ has branch points. The problem has already been evoked and partially solved about the Burgers equation, i.e., (1.1) without the integral term, by Bessis and Fournier [44] who showed that an entire initial condition may immediately evolve to a pole-decomposed form. In the case of (7.2) or the MS equation, however, nothing is yet known [no Hopf-Cole transform [45] is yet available for (1.1) or (4.9)].

A second, physical argument in favor of the pole-decomposable solutions is that they are able to describe (via the MS equation) the structure of a flame that is planar on average [29], as a spherical flame is locally when $\tau \to \infty$; it is then difficult to understand why they should be unable to describe the transition between $\tau = O(1)$ and $\tau = \infty$, given that they also qualitatively imitate what normal-mode analyses give in cases of small amplitude. Equation (7.2) itself could be structurally unable to produce the phenomenon of cell splitting: a way to check this hypothesis would be to integrate (7.2) by a spectral or pseudospectral method and to compare the results with what pole motions give; this is the subject of current works [46]. One has to remember that such numerical methods, though very accurate, are not noise free when implemented in an actual computer, a fact that could have misleading consequences (see Sec. VI A, or Ref. [17]); this remark can possibly explain why [47] recently succeeded in reproducing repeated cell splitting.

(2) It could be that any realistic dynamics deduced from (7.2) has to involve an infinite number of poles (per $2\pi/K$ cell). Since poles cannot crop up from a smooth, bounded analytic function (again according to Liouville's theorem), these infinitely many singularities must be present at $\tau = \tau_0^+$. This possibility is compatible with both the aforementioned analysis of [44] and with the presumably irregular, fractal-like structure of any realistic, experimental initial condition. Actually, the conceivable problems due to the finiteness of N were somehow already present in the linear, normal-mode analysis presented in Sec. VI A: in order that an endless cell splitting be envisaged, *all* the normal modes, including the highest angular harmonics, had to be initially present. Sometimes, nonlinearity is sufficient for continuously generating harmonics of arbitrarily high orders, thereby allowing for a transient subsequent amplification once they are stretched [35]; in the present case this argument does not function, at least within the class of pole-decomposable solutions. One clearly understands, however, that using $N = \infty$ in (7.5) leads to noticeable difficulties. A way to test the above ideas would be to integrate (7.5) (with larger and larger values of N so as to account for the finer and finer initial details of the initial flame shape) and then to extrapolate the results to $N = \infty$. Obviously, commuting the limits $N \to \infty$ and $\tau \to \infty$ is a very delicate matter; unfortunately, it is possibly the only one that really matters.

(3) A "square," curvilinear domain of integration could be inadequate. To make the study of (4.9) easier, we assumed periodic boundary conditions and a square integration domain; then we used a separation of variables. It is known, however, that hexagons often lead to different bifurcation diagrams from those pertaining to square or one-dimensional patterns (e.g, see [48] and to different mode-mode couplings. Even though a few transient, hexagonal solutions to the two-dimensional Burger's equation can be constructed analytically upon use of the hopf-Cole trick, we have so far been unable to

do the same thing for the MS equation or (4.9). On the other hand, this author does not know how to use spectral methods to integrate (4.9) on an hexagonal domain, so that exploiting the possibilities implied by (3) remains an open problem.

(4) External noise, even if of a very small intensity, would be needed for theory to agree qualitatively with reality. It is difficult to imagine why this noise should be compatible with the large-scale, angular periodicity corresponding to an $O(1)$, but otherwise arbitrary, sector; instead a fixed, small-scale, average spatial size is expected, especially if the noise has a hydrodynamic origin (one must note, however, that finding the way the blast flow induced by expansion affects an initially isotropic, small-scale turbulence is a problem that has yet to be solved). The linear analyses reported in Secs. IV A and X tend to suggest that such a noise does have a strong influence. Since the angular and spatial periodicities are in general incompatible (due to the identity $X=\sigma\tau$ and to the *continuous* growth of τ), testing this idea with pseudospectral methods could lead to computational difficulties, unless a markedly broadbanded noise is employed or the whole flame surface is handled.

There is yet another way of accounting for an external noise that would present the above characteristics on average: it consists of still using (7.4) and (7.5), but with a time-dependent, increasing number of poles $N(t)$. Though apparently exotic, this procedure has been previously proposed as a mathematical trick to study the response of a "planar" unstable flame to a weakly "turbulent" incoming flow [49]; one may thus envisage using it here as well. In the present context, this would amount to studying the following nonhomogeneous version of (7.2):

$$F_\tau+\frac{1}{2\tau^2}F_\sigma{}^2=\frac{\mu}{2\tau^2}F_{\sigma\sigma}+\frac{1}{\tau}I(F,Z)+u_e(\tau,\sigma)\ , \qquad (12.1)$$

where $u_e(\tau,\sigma)$—the noise—satisfies $\langle u_e\rangle=0$ and is given by

$$u_e(\tau,\sigma)=\sum_m \delta(\tau-\tau_m)[\psi_m(\sigma)-\langle\psi_m\rangle]\ ,$$
$$\psi_m(\sigma)=-2\mu\ln[1-\cos K(\sigma-A_m)\operatorname{sech}KB_m]\ . \qquad (12.2)$$

In (12.2), $0\le A_m<2\pi/K$, $B_m>0$, and $\tau_m>0$ ($m=0,1,\ldots$) are independent, and possibly *random*, arbitrary parameters. This seemingly complicated formulation is readily understood once one realizes that the influence of the above shot-noise-like $u_e(\tau,\sigma)$ is merely to implant new poles ($A_m\pm iB_m$) at given times, without changing the structure of (7.3) and (7.5) between the implants; only N changes, of course, stepwise. When $B_m\gg1$, $\psi_m(\sigma)$ is a small-amplitude, near-harmonic function [see (8.5)]; A_m controls its phase and B_m the amplitude. In a sense, (12.1) and (12.2) are a nonlinear analog of (6.7). By contrast to the interesting numerical work of Chaté [50], which also involved random sequences of rapid flame distortions and then of free propagation, the above model also includes some features of the intrinsic flame instability. Upon use of an adequate rate of pole sparkling (via the τ_m's) and of adequately sampled phases (the A_m's), the above model can possibly statistically reconcile the periodicity in σ and the existence of a constant wavelength of u_e. Equations (12.1) and (12.2) thus lead to a mathematical model to study the response of expanding flames to turbulentlike incoming fluctuations; in such a formulation, the flame dynamics would result from a competition between crest coalescence (i.e., pole alignment) and crest nucleation (due to noise). Given the differences, displayed in Sec. VI, between an initial value problem and forced dynamics, this model is worth studying, e.g., in connection with Palm-Leis and Strehlow's statement quoted at the beginning of this section. It is yet unclear, however, whether the average cell size (if any) will be fixed by intrinsic characteristics of the mixture (as Sec. VI A suggests) or by the noise properties (see Secs. VI B and X). As a further indication, which tends to suggest that the influence of an external noise is, in a sense, similar to adding poles, we consider the following nonhomogeneous MS equation:

$$\phi_\tau+\tfrac{1}{2}\phi_X{}^2=\mu\phi_{XX}+I(\phi,X)+u_e(\tau)\cos(k_eX)\ , \qquad (12.3)$$

for the sake of illustration and briefly analyze how a naive operator-splitting numerical method would handle it between τ and $\tau+\delta\tau$ ($\delta\tau\ll1$). A first step (the influence of pure noise) would increase ϕ *jumpwise* by an amount $u_e(\tau)\delta\tau\cos(k_eX)$, thereby leading to the intermediate shape ϕ_*; a second step would allow the flame shape ϕ to relax *freely* (i.e., under the sole influences of curvature, nonlinearity, and Landau-Darrieus instability) from ϕ_* to $\phi(\tau+\delta\tau,X)$. The first step is analogous to the addition of a pair of remote poles $A\pm iB$, with

$$4\mu\exp(-k_eB)\cong|u_e|\delta\tau$$

and $k_eA=0$ if $u_e>0$, or $k_eA=\pi$ if $u_e<0$, because numerical methods do not really allow one to know what effectively happened to the physics between τ and $\tau+\delta\tau$; the second step clearly corresponds to the free dynamics (8.5). According to the above interpretation, a forcing term (here, $u_e\cos k_eX$) would be equivalent to a source of infinitely many, infinitely remote ($\delta\tau\to0$) poles. Though we do not yet have definitive answers, it is readily conceived that adding poles (explicitly or indirectly via a noise) is likely to allow for an endless cell splitting of expanding fronts, since the number of "available ridges" would no longer be bounded. At any rate, the importance of noise in expanding flame dynamics should be accurately assessed.

The above possibilities are the subject of current works [46], whose results will be published in due course. We do realize that pole decompositions are not a panacea; nevertheless, following Bender and Orszag [45] (p.61), we do hope that "singularity almost invariably is the clue," at least to our understanding the way the flames behave. At any rate the method will furnish valuable, benchmark results for alternative procedures. The duality poles–Fourier-modes could also be a valuable guide to intuition. Moreover, even if refinements of the MS equation and its generalization are needed (e.g., see [51]), it is

not obvious at all why the pole-decomposition method should cease to be useful [52].

Our final remark is to emphasize that steadily expanding flames (radius proportional to τ^{ω}, $\omega=1$) are rather peculiar objects: any faster growth ($\omega>1$) would tend to inhibit the Landau-Darrieus linear-instability, because $1/\tau^{\omega}$ would then be integrable at $\tau=\infty$, thereby ultimately leading to $\omega=1$ in the absence of noise; on the other hand, a slower growth ($\omega<1$) could result in an exponential growth of wrinkles, and hence in a self-acceleration. This tends to somewhat moderate the conclusions drawn in [34] about the mechanism of self-acceleration of large-scale expanding flames ($\omega\cong\frac{3}{2}>1$, according to their experiments). However, one must not forget the ever present sources (e.g., thermal) of noise, and acknowledge that acceleration ($\omega>1$) enhances instability through buoyancy effects (these do not show up at the leading orders in the limit $\gamma\to 0$) that could *dominate* the Landau-Darrieus mechanism in the long-wavelength limit, but would vanish as $\tau\to\infty$ if $\omega<2$. It is therefore not totally excluded that small external fluctuations or thermal noise and buoyancy induced by acceleration are able to maintain an expanding flame in a regime of slightly accelerated propagation but, clearly, even this innocuous looking problem of a "freely" expanding flame deserves further studies. More generally, this suggests that the influence "of small scales on larger ones," which the renormalization procedures [34,54] currently try to account for, has to be complemented in the context of moderately turbulent flames by more "mean-field" ingredients, because large-scale behaviors may modify the local flame dynamics significantly in the limit of long times.

ACKNOWLEDGMENTS

The author is greatly indebted to Dr. P. Cambray (Poitiers University) for his invaluable aid in the numeric-related topics, especially about Figs. 12 and 13, and to Professor G. I. Sivashinsky for enjoyable and stimulating conversations. Dr. J. W. Dold and K. Joulain are also thanked for discussions. This work was performed as a partial fulfillment of the DRET/ENSMA Contract No. 93-060. The Laboratoire d'Energétique et Détonique is "Unité de recherche associée au CNRS No. 193."

[1] G. I. Sivashinsky, Annu. Rev. Fluid Mech. **15**, 179 (1983).
[2] G. I. Sivashinsky, Philos. Trans. R. Soc. London, Ser. A **332**, 135 (1990).
[3] P. Clavin, Prog. Energy Combust. Sci. **11**, 1 (1985).
[4] F. A. Williams, *Combustion Theory* (Benjamin Cummings, Menlo Park, CA, 1985).
[5] Ya B. Zel'dovich, G. I. Barenblatt, V. B. Librovich, and G. M. Makhviladze, *The Mathematical Theory of Combustion and Explosions* (English translation) (Consultants Bureau, New York, 1985).
[6] L. D. Landau, Acta Physicochim. **19**, 77 (1944).
[7] G. Darrieus (unpublished).
[8] G. I. Sivashinsky, Acta Astronautica **4**, 1177 (1977).
[9] G. I. Sivashinsky and P. Clavin, J. Phys. (Paris) **48**, 193 (1987).
[10] E. Ott and R. N. Sudan, Phys. Fluids **12**, 2388 (1969).
[11] E. Ott, W. M. Manheimer, D. L. Book, and J. P. Boris, Phys. Fluids **16**, 855 (1973).
[12] D. M. Michelson and G. I. Sivashinsky, Acta Astronautica **4**, 1207 (1977).
[13] Ya B. Zel'dovich, B. Istratov, A. G. Kidin, and V. B. Librovich, Combust. Sci. Technol. **24**, 1 (1980).
[14] P. Pelcé and P. Clavin, Europhys. Lett. **3**, 907 (1987).
[15] P. Pelcé, *Dynamics of Curved Fronts* (Academic, New York, 1989).
[16] B. Denet, thesis, University of Provence, Marseille, 1988.
[17] G. Joulin, J. Phys. (Paris) **50**, 1069 (1989).
[18] S. Gutman and G. I. Sivashinsky, Physica D **43**, 129 (1989).
[19] A. Palm-Leis and R. A. Strehlow, Combust. Flame **13**, 111 (1969).
[20] E. G. Groff, Combust. Flame **48**, 51 (1982).
[21] T. A. Baritaud, in *Turbulent Reactive Flows,* edited by R. Borghi and S. N. B. Murthy, Lecture Series in Engineering Vol. 40 (Springer-Verlag, New York, 1989), pp. 81–92.
[22] A. G. Istratov and V. B. Librovich, Astronaut. Acta **14**, 453 (1969).
[23] J. K. Bechtold and M. Matalon, Combust. Flame **67**, 77 (1987).
[24] M. D. Kruskal, in *Nonlinear Wave Motion,* edited by A. Newell (American Mathematical Society, Providence, 1974), pp. 61–83.
[25] M. J. Ablowitz and H. Segur, *Solitons and the Inverse-scattering Method,* SIAM Studies in Appl. Math. (Philadelphia, 1981).
[26] Y. C. Lee and H. H. Chen, Phys. Scr. **T2**, 41 (1982).
[27] O. Thual, U. Frisch, and M. Henon, J. Phys. (Paris) **46**, (1985).
[28] G. Joulin, Combust. Sci. Technol. **53**, 315 (1987).
[29] G. Joulin and P. Cambray, Combust. Sci. Technol. **81**, 243 (1992).
[30] G. H. Markstein, *Nonsteady Flame Propagation* (Pergamon, New York, 1964).
[31] P. Clavin and G. Joulin, J. Phys. (Paris) Lett. **1**, L1 (1983).
[32] P. Cambray, B. Deshaies, and G. Joulin (unpublished).
[33] P. Clavin and G. Joulin, in *Turbulent Reactive Flows,* edited by R. Borghi and S. N. B. Murthy, Lecture Series in Engineering Vol. 40 (Springer-Verlag, New York, 1989), pp. 213–239.
[34] Yu. A. Gostinsev, A. G. Istratov, and Yu. V. Shulenkin, Combust. Expl. Shock Waves **24**, 563 (1989).
[35] G. I. Sivashinsky, C. K. Law, and G. Joulin, Combust. Sci. Technol. **22**, 155 (1982).
[36] J. O. Hinze, *Turbulence* (McGraw-Hill, New York, 1959).
[37] P. Pelcé and P. Clavin, J. Fluid Mech. **124**, 219 (1982).
[38] G. Searby and D. Rochwerger, J. Fluid Mech. **231**, 529 (1991).
[39] P. Garcia-Ybarra, C. Nicoli, and P. Clavin, Combust. Sci. Technol. **42**, 87 (1984).
[40] M. Renardy, Physica D **28**, 155 (1987).
[41] S. S. Minaev, Combust. Expl. Shock Waves **28**, 30 (1992).
[42] H. V. McConnaughey, G. S. S. Ludford, and G. I. Sivashinsky, Combust. Sci. Technol. **33**, 113 (1983).
[43] E. Goursat, *Traité d'Analyse Mathématique* (Gauthier-

Villars, Paris, 1912).
[44] D. Bessis and J. D. Fournier, J. Phys. (Paris) Lett. L833–L841 (1984).
[45] C. M. Bender and S. A. Orszag, *Advanced Mathematical Methods for Scientists and Engineers* (McGraw-Hill International Book Company, Auckland, 1984).
[46] P. Cambray and G. Joulin (unpublished).
[47] L. Filyand, G. I. Sivashinsky, and M. L. Frankel (private communication).
[48] D. H. Sattinger, *Cooperative Effects in Fluid Problems,* in Synergetics: A Workshop, edited by Haken (Springer-Verlag, New York, 1977), pp. 51–57.
[49] G. Joulin, Combust. Sci. Technol. **60**, 1 (1988).
[50] H. Chaté, in *Mathematical Modelling in Combustion and Related Topics,* Vol. 140 of *NATO Advanced Study Institute, Series E,* edited by C-M. Brauner and C. Schmidt-Lainé (M. Nijhoff, Dordrecht, 1988), pp. 441–448.
[51] S. K. Zhdanov and B. A. Trubnikov, Sov. Phys. JETP **68**, 65 (1989).
[52] G. Joulin, Zh. Eksp. Teor. Fiz. **100**, 428 (1991).
[53] M. L. Frankel, Phys. Fluids A **2**, 1879 (1990).
[54] V. Yakhot, Combust. Sci. Technol. **60**, 191 (1988).